Particle in cell/Monte Carlo collision analysis of the problem of identification of impurities in the gas by the plasma electron spectroscopy method

C. Kusoglu Sarikaya,[1] I. Rafatov,[1,a)] and A. A. Kudryavtsev[2]
[1]*Department of Physics, Middle East Technical University, 06800 Ankara, Turkey*
[2]*Saint Petersburg State University, St. Petersburg, Russia*

(Received 11 April 2016; accepted 14 June 2016; published online 29 June 2016)

The work deals with the Particle in Cell/Monte Carlo Collision (PIC/MCC) analysis of the problem of detection and identification of impurities in the nonlocal plasma of gas discharge using the Plasma Electron Spectroscopy (PLES) method. For this purpose, 1d3v PIC/MCC code for numerical simulation of glow discharge with nonlocal electron energy distribution function is developed. The elastic, excitation, and ionization collisions between electron-neutral pairs and isotropic scattering and charge exchange collisions between ion-neutral pairs and Penning ionizations are taken into account. Applicability of the numerical code is verified under the Radio-Frequency capacitively coupled discharge conditions. The efficiency of the code is increased by its parallelization using Open Message Passing Interface. As a demonstration of the PLES method, parallel PIC/MCC code is applied to the direct current glow discharge in helium doped with a small amount of argon. Numerical results are consistent with the theoretical analysis of formation of nonlocal EEDF and existing experimental data. *Published by AIP Publishing.*
[http://dx.doi.org/10.1063/1.4954917]

I. INTRODUCTION

Study of glow discharge plasmas is important due to their numerous technological applications in surface modification, plasma light sources, plasma medicine, TV displays, etc.[1] Nowadays, computer simulations of low-temperature plasmas are widely used in both research institutions and industry.[2] However, a discrepancy between the simulation results and experimental evidence may cast some doubt upon the usefulness of the simulation results. This underlines the need for the understanding of the capabilities and limitations of the models and of the main physics governing a particular discharge.

Modelling approaches commonly used in practice may be classified in the fluid, kinetic/particle, and hybrid methods.[2] The fluid models are the most popular due to their relative ease of implementation and computational efficiency. However, fluid models are inapplicable to the short discharges (in terms of the product pL of the pressure p and the characteristic plasma length L) with nonlocal electron energy distribution function (EEDF) when the characteristic length L is less than the electron energy relaxation length, $L < \lambda_\varepsilon$. In the elastic energy region $\varepsilon < \varepsilon^*$ (where ε^* is the threshold energy), this length is rather large

$$\lambda_\varepsilon = \lambda/\sqrt{\delta} > 100\lambda \tag{1}$$

(for details, see, e.g., Ref. 3). Here, λ is the electron free mean path and $\delta = 2m_e/M$ is the ratio of the electron mass to the heavy particle mass. If $L < \lambda_\varepsilon$, EEDF is nonlocal because transversal diffusion of electrons occurs more effectively than the change in their energy in the plasma volume. As a result, the EEDF is determined by the plasma parameters in the region of the dimension λ_ε rather than by the local parameters of the plasma in a given point of space.[3] Estimations revealed that plasma of atomic gases is nonlocal up to the values $pL < 10$ cm Torr that comprises not only low and medium pressure discharges but also microdischarges at high pressures.[3]

Recall that there are two basic scenarios of formation of the nonlocal EEDF in low pressure gas discharges.[3] The main part of the electrons (the bulk electrons, which constitute the plasma density) is trapped in the volume by the ambipolar field and the near-wall sheath potential drop. Another group of electrons from the tail of the EEDF with energies $\varepsilon > e\Phi_\omega$ (Φ_ω denotes the potential drop between the central region of plasma and its border) leave rapidly the bulk of the plasma towards the walls or/and electrodes by free diffusion so that their density in the plasma is rather low.

If nonlocal plasma is autonomous (supported by its own electric field, as, e.g., in the positive column of the glow discharge), the electron temperature T_e is sufficiently high and $e\Phi_\omega$ is greater than the ionization potential ε_{ioniz}, $e\Phi_\omega > \varepsilon_{ioniz}$, because the electron losses on the walls must be compensated by their birth in the ionization processes.[3] In this situation, trapped electrons occupy a wide range of energies and an exploration of their EDF is of primary concern because it determines all basic parameters of interest of nonlocal plasma. The main difference from the local regime is that the argument of EDF of nonlocal trapped electrons represents the total energy $\varepsilon = mV^2/2 + e\varphi(\mathbf{r})$ (the sum of kinetic and potential energies) and hence does not depend on the spatial coordinates explicitly. Presently, basic features of nonlocal EDF of trapped electrons have been studied both theoretically and experimentally (see, e.g., Ref. 3 for details).

In the opposite situation, when ionization in the plasma is sustained by the external sources, temperature T_e of

a)Electronic mail: rafatov@metu.edu.tr

trapped electrons (as well as the potential drop Φ_ω which is of the order of several T_e/e) is low. As a consequence, electrons with energies $\varepsilon > e\Phi_\omega$ of several electron volts move freely towards the walls, while their total energy remains practically unchanged by collisions. Plasma of the negative glow region of glow discharge, sustained by the beam of electrons from the cathode layer (more generally, negative-glow-like plasmas according to the terminology in Refs. 4 and 5), provides an example of this situation.

Investigation of EDF of free (untrapped) nonlocal electrons in nonlocal plasma is important for both basic and applied research. One of the applications exploiting the behavior of this electron group is the method that was called the Plasma Electron Spectroscopy (PLES) in Ref. 6. The idea of this method is based on the analysis of the effect on the EEDF due to electrons, released in the Penning reactions between the metastable atoms of working gas (He) and impurity (A)

$$\mathrm{He}^* + \mathrm{A} \rightarrow \mathrm{He} + \mathrm{A}^+ + e_\mathrm{P}. \tag{2}$$

Here, the Penning electron's energy ε_P is

$$\varepsilon_\mathrm{P} = \varepsilon_\mathrm{met} - \varepsilon_\mathrm{ioniz}, \tag{3}$$

where ε_met is the excitation energy of the metastable particle He^* and $\varepsilon_\mathrm{ioniz}$ is the ionization energy of the impurity A. Employing helium as a working gas is preferable because its excitation energy is greater than the ionization energy of any other gas except neon.

The energy spectra of the Penning electrons produced in the reaction (2) represents sharp peaks in the EEDF about the release energy ε_P (3) of the Penning electrons.[6] Therefore, given the measured energy of the peaks of these electrons, the ionization energy $\varepsilon_\mathrm{ioniz}$ of the particles A can be obtained from Equation (3) and thereby the impurity atoms or molecules can be identified. Moreover, given the measured density of Penning electrons and the well-known rate constants for the Penning reaction (2), the densities of the impurities can be determined as well.

The PLES method has been explored experimentally in Refs. 7–10. Further advance in the PLES requires development of the reliable numerical models and carrying out numerical simulations, which will provide useful insight into the applicability and limitations of this method and optimization of its operational parameters. However, detailed numerical analysis related to PLES has not been done yet. Since EDF of nonlocal electrons with energies $\varepsilon > e\Phi_\omega$ is a function of both the energy and the spatial coordinates, modelling of EDF in this plasma and interpretation of the results presents a severe problem. Indeed, self-consistent description of nonlocal plasma must involve solution of the kinetic Boltzmann's equation for EEDF in the domain of the electron energy and space coordinates, which poses a severe challenge to the numerical model.

Therefore, to model properly gas discharges with nonlocal EEDF, kinetic method should be used. Method of particles such as PIC/MCC (Particle in Cell/Monte Carlo Collision) has proved to be a convenient way of doing this. Since PIC/MCC simulation allows to develop profiles of the energy distribution functions $f_\mathrm{k}(\mathbf{r}, \mathbf{v}, t)$ of plasma species, it may be classified as (statistical) method of solution of Boltzmann's kinetic equation

$$\left[\frac{\partial}{\partial t} + \mathbf{v}\cdot\nabla_r + \mathbf{a}\cdot\nabla_v\right] f_\mathrm{k} = \left(\frac{\delta f_\mathrm{k}}{\delta t}\right)_{\mathrm{coll.}}. \tag{4}$$

More specifically, PIC/MCC method includes solution of Lorentz equations of motion to determine the positions and velocities of each individual particle and the Maxwell's equation to determine the electromagnetic fields. The MCC method is used for analyzing collisions between particles. In order to reduce the numbers of particles to tractable order, PIC/MCC method employs the concepts of "super particle," which represents huge number of actual particles (usually of the order 10^4–10^6) in the plasma. There are various techniques developed to speed up the PIC computations, e.g., the ion subcycling, the null collision method, etc.[11,12] Since 1990s parallel computing[13–15] improving significantly performance of the PIC/MCC simulations is an active area of research.

In the present work, we carried out 1d3v parallel PIC/MCC analysis of glow discharge plasma in the mixture of helium and argon, related to the problem of identification of impurities in the gas within the PLES method.[6–10] Description of the PIC/MCC model is given in Section II A. The verification of the numerical code is done in Section II B. In order to increase the efficiency of the method, the code is parallelized and the effect of parallelization on the performance is discussed in Section II C. Application of the code to the problem of detection and identification of the impurities by PLES method is studied in detail in Section III. Finally, conclusions are presented in Section IV.

II. PIC/MCC MODEL

A. Method

As an approach leading to determination of the energy distribution functions of the plasma species, PIC/MCC can be classified as kinetic method. It operates with superparticles, representing large amounts of real particles. The concept of superparticle helps handle with reasonable order of particles in the simulation. Furthermore, introduction of the computational grid ("cells") simplifies calculation of the electric and magnetic fields and their addressing to superparticles.

PIC/MCC simulation cycle is summarized as follows. First, particles are assigned to the grid points; the charge density at the grid points is evaluated. Second, the electric field profile responding to the charge distribution is computed from the Poisson equation

$$-\epsilon_0\nabla^2\phi = \rho. \tag{5}$$

Then, effect of the Lorentz force $\mathbf{F} = q\mathbf{E}$ is interpolated to the particles (magnetic field is ignored in this study). Next, positions and velocities of the particles are updated from the solution of the equations of motion. By the Leapfrog method,

with Δt denoting the time step and index k denoting the time level,

$$v_{k+1/2} = v_{k-1/2} + \frac{F(x_k)\Delta t}{m}, \tag{6}$$

$$x_{k+1} = x_k + v_{k+1/2}\Delta t. \tag{7}$$

Finally, the MCC method is applied to account for the effect of boundaries and collisions of particles. Particles can be either absorbed or reflected or cause to emit secondary electrons from the boundaries. Elastic scattering, ionization, and excitation collisions between electrons and neutrals and isotropic scattering and charge exchange between ions and neutrals are taken into account. The "null collision" method[12] is applied to speed up the MCC procedure. Colliding particles which number is defined as a product of the total number of superparticles with the collision probability

$$P = 1 - \exp(-n\sigma_t v\Delta t) \tag{8}$$

are selected randomly. Here, n is the neutral density, σ_t is the total cross section, and v is the velocity of particle. Actual collision type for each colliding particle is determined from the correlation of the ratio of the reaction cross-sections to the total cross-section, σ_k/σ_t, with the random numbers distributed uniformly between 0 and 1. Then, the cycle is repeated on the new time level.

There are restrictions imposed on the time and space steps. The space step must not exceed the Debye length, while the time step is limited by the Courant condition and the plasma oscillation frequency. Moreover, in order to provide accurate and statistically relevant results, there must be sufficient number of superparticles per Debye length that places limitations on the weighting of superparticles. For details of the method, see, e.g., Refs. 17 and 18.

B. Verification of the PIC/MCC code

We carried out benchmark test by adopting our 1d3v PIC/MCC code to the conditions in Ref. 19 for Radio-Frequency (RF) capacitively coupled discharge in helium. One of the electrodes is grounded, and the other is driving with sinusoidally varying voltage,

$$V = V_0 \sin(2\pi ft). \tag{9}$$

Initially, electrons and ions over the discharge gap were located randomly according to the uniform distribution, while their velocities were chosen according to the Maxwell distribution,

$$\mathbf{v} = \sqrt{-\log(R_1)2k_BT/m}\,\sin(2\pi R_2). \tag{10}$$

In this equation, k_B is the Boltzmann constant, T is the temperature (in K), m is the particle mass, and R_1 and R_2 are uniform random numbers defined between 0 and 1. Secondary electron emission and reflection from the electrodes were ignored in this test.[19] Elastic collisions, singlet excitation, triplet excitation, and direct ionization collisions were taken into account between electrons and neutrals, and isotropic scattering and charge exchange between ions and neutrals. We used collision cross-sections for electron-neutral pairs (Fig. 1) from the Biagi database.[16] For the collisions between ions and neutrals, cross-sections of the isotropic and backward scattering were defined as[20]

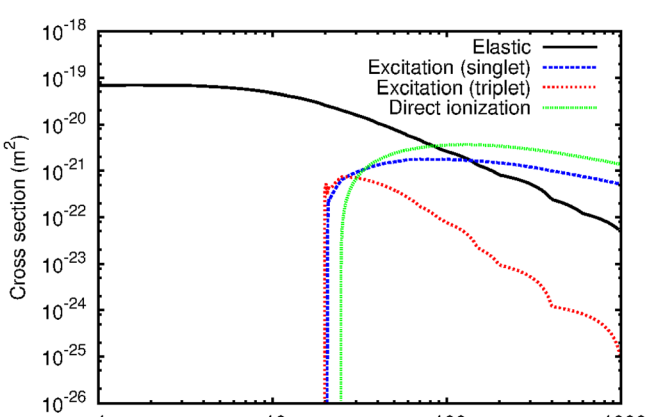

FIG. 1. Electron cross-sections for elastic, excitation, and direct ionization collisions in helium used in the model.[16]

$$\sigma_{iso} = 7.63 \times 10^{-20}(E_{rel}^{-0.5})\,\mathrm{m}^2, \tag{11}$$

$$\sigma_{back} = 10^{-19}(10^{-3}E_{rel})^{-0.15} \times (1 + 10^{-3}E_{rel})^{-0.25}(1 + 5E_{rel}^{-1})^{-0.15}\,\mathrm{m}^2. \tag{12}$$

Here, E_{rel} denotes the relative energy of ion respective to the neutral particle energy (in eV).

The parameters used in the test simulations are summarized in Table I. The simulation lasts for 10^{-4} s with time step 10^{-10} s. To optimize the code, the "null collision" method[12] and the subcycling of ions[11] are used. Comparison of the profiles of computed power density and ion density with those from Ref. 19 demonstrated in Fig. 2 supports to the validity of the numerical code.

C. Parallelization of the PIC/MCC code

Parallelization of the code is an effective way to improve the efficiency of the numerical model. We used Open MPI (Message Passing Interface).[21] The effect on the performance of the model was analyzed as function of the number of cores involved in the parallel calculations, by increasing that up to 95. Test simulations were carried out for the RF capacitively coupled discharge in helium. On the boundaries, secondary electron emission from the cathode

TABLE I. The parameters in test simulations of capacitively coupled RF discharge.[19]

Voltage (V)	450
Discharge gap (cm)	6.7
Frequency (MHz)	13.56
Pressure (Pa)	4
Weighting	2.6×10^8
Number of grid points	128

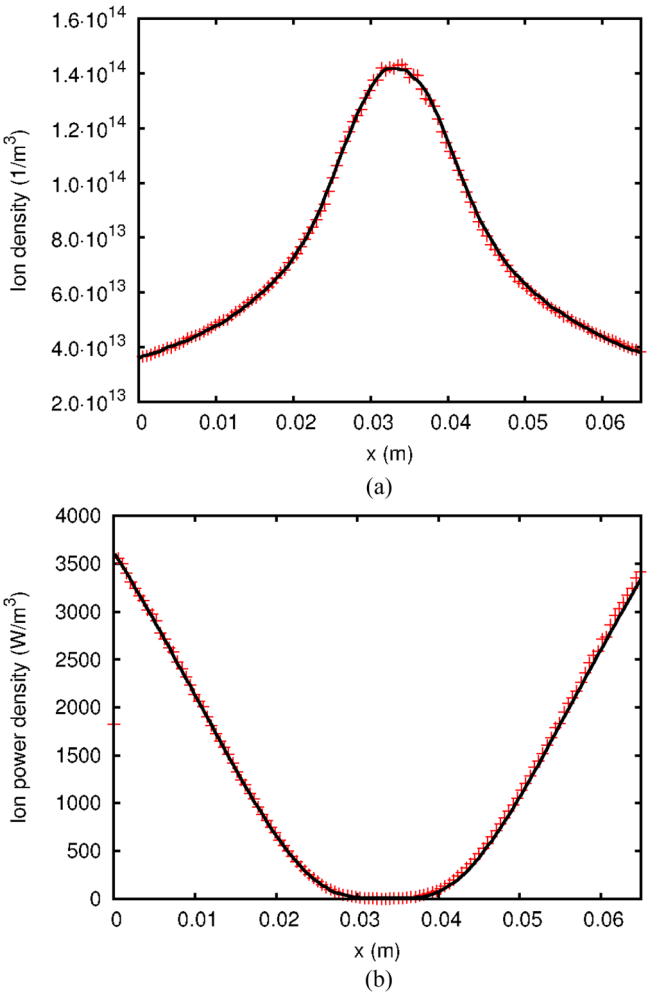

FIG. 2. Ion (a) and power densities (b). Solid line corresponds to the result from Ref. 19. Conditions are given in Table I.

and reflection of electrons from the anode were taken into account. Parameters, which we used in this analysis, are summarized in Table II.

Figure 3 illustrates the overall effect of the number of cores as well as their effect on the basic modules of the parallel code. As can be seen from this figure, the most time consuming component of the code is MCC module. The gain in the overall performance is about 70 times when using 95 cores. It can be noted that with the increase in the number of cores, the rate of decrease in the "elapsed time" slows down. The main reason is the nonuniformity of the loads imposed on the cores that becomes noticeable in this case.

TABLE II. The parameters used in the parallelization test.

Voltage (V)	500
Discharge gap (cm)	4
Frequency (MHz)	1.5
Pressure (Pa)	46
Secondary electron emission coefficient, γ	0.3
Reflection coefficient, r	0.25
Weighting	3.0×10^7
Number of grid points	600

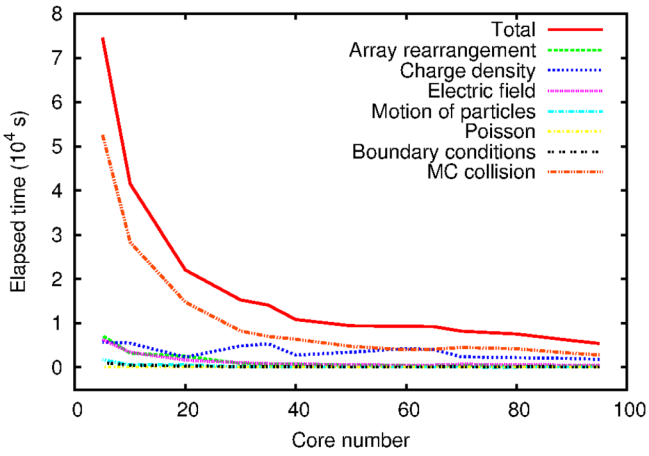

FIG. 3. Efficiency test for parallel PIC/MCC code. Results shown correspond to the range from 5 to 95 core numbers. Conditions are given in Table II.

III. APPLICATION OF THE CODE TO THE PLASMA ELECTRON SPECTROSCOPY (PLES) METHOD

As it was indicated in the Introduction, the new method known as the Plasma Electron Spectroscopy (PLES) for the identification of impurities in gases was proposed in Ref. 6. This method is an alternative to the high-vacuum devices used in classical electron spectroscopy.

For the practical implementation of the analysis of impurities by PLES method, it is essential that each group of Penning electrons arrive at the analyzer, while their release energy (3) remains unchanged. This implies that the electrons do not "mix" due to collisions in the course of their motions towards the boundaries of the plasma volume, that is the condition of formation of nonlocal EEDF. Indeed, with condition (1)

$$\lambda_\varepsilon = \lambda/\sqrt{\delta} > 100\lambda$$

is satisfied, different groups of electrons with energy $\varepsilon > e\Phi_\omega$ behave independently and reach at plasma boundaries keeping their total energy practically constant.[3] Here, λ is the electron free mean path, λ_ε is the electron energy relaxation length, $\delta = 2m_e/M$ is the ratio of the electron mass to the heavy particle mass, and Φ_ω is the potential drop between the discharge axis and the wall. According to the analysis of formation of nonlocal EEDF,[6] in the absence of the electric field or when it is weak (e.g., in negative glow plasma, in afterglow plasma, where the electron temperature T_e and hence $e\Phi_\omega$ is small), the EDF of Penning electrons exhibits sharp peaks near the energies ε_P, reproducing the narrow spectrum of the Penning electrons released in the reactions (2).

Experimental verification of these estimations in Refs. 7–10 was concerned with the study of short (without positive column) glow discharges in helium doped with small amount of impurity gases. These measurements, indeed, revealed the peaks in the second order derivatives of the probe currents precisely about the energy values determined by Equation (3). This effect can be employed to identify the impurities, and hence, it provides an opportunity for PLES applications.

However, further development of PLES requires knowledge of the applicability limits of this method and optimization of its operational parameters. Therefore, it is very desirable to have reliable simulation results regarding the relevant gas discharge facilities. It is appropriate to recall that numerical methods based on the fluid models are not applicable in this case because the local EDF for Penning electrons within these models represents not the peaks but the step-like profiles in the region of their release energy.[6] In order to reproduce the experimental conditions properly, self-consistent simulation of nonlocal plasma of the gas discharge must involve solution of the kinetic Boltzmann equation for electrons in both energy and spatial coordinate domains.

In this work, we followed typical experimental conditions of Refs. 7–10 for the case of the direct current (DC) glow discharge sustained in the mixture of helium and 0.2% of argon. Penning ionization reactions expected between the metastable (singlet and triplet) helium atoms and argon atoms are

$$\mathrm{He}^*(2^3\mathrm{S}_1) + \mathrm{Ar}(0) \rightarrow \mathrm{He}(0) + \mathrm{Ar}^+(^2p_{3/2}) + e_\mathrm{P}(4.06\,\mathrm{eV}), \tag{13}$$

$$\mathrm{He}^*(2^1\mathrm{S}_0) + \mathrm{Ar}(0) \rightarrow \mathrm{He}(0) + \mathrm{Ar}^+(^2p_{3/2}) + e_\mathrm{P}(4.85\,\mathrm{eV}). \tag{14}$$

We used cross-sections of collisions between electrons and neutrals given in Fig. 1 and cross-sections of collisions between ions and neutrals defined by Equations (11) and (12). Processes of multistep ionization and Coulomb collisions were ignored because nonlocal weakly ionized plasma with degree of ionization and excitation less than 10^{-6} was considered. Moreover, we incorporated PIC/MCC numerical model with equations for density of the metastable (single and triplet) helium atoms in the fluid approximation,

$$\frac{\partial n}{\partial t} - D\,\frac{\partial^2 n}{\partial x^2} = S, \tag{15}$$

where D is the diffusion coefficient and S is the excitation source term. At the boundaries, metastable helium atoms were assumed to be absorbed. The diffusion coefficient was computed from[22]

$$D = (420/p) \times (T_\mathrm{g}/0.025)^{1.5}\,\mathrm{cm^2 s^{-1}}, \tag{16}$$

where T_g is the gas temperature in eV and p is the pressure in Torr. Penning ionization cross sections in the mixture of helium and argon were taken as 16.4×10^{-16} cm^2 and 5.3×10^{-16} cm^2 for the singlet and the triplet metastable He atoms, respectively.[23]

TABLE III. The parameters used in the PLES simulation.

Voltage (V)	400
Discharge gap (cm)	0.4
Pressure (Pa)	753
Secondary electron emission coefficient, γ	0.15
Reflection coefficient, r	0.2

TABLE IV. The numerical parameters employed for the PLES simulation. $t = 1.4 \times 10^{-5}$ s. Debye length λ_D and number of super electrons per Debye length N_D correspond to the point where the electron density is greatest.

Weighting	1.6×10^8
Number of grid points	1333
Total number of superelectrons	1 518 360
Average number of superelectrons per grid cell	1139
Debye length, λ_D (m)	2.73×10^{-6}
N_D	1025

The parameters used in this simulation are summarized in Tables III and IV. The values of the total number of super electrons, average number of super electrons per grid cell, Debye length, λ_D, and number of super electrons per Debye length, N_D, correspond to $t = 1.4 \times 10^{-5}$ s. Parameters λ_D and N_D were computed at the position of maximum electron density.

As can be seen from Fig. 4, about 2×10^6 time steps are required to settle the discharge down to the steady state (this corresponds to the "physical" time interval of 2×10^{-5} s).

Figure 5 demonstrates the electric potential and electric field profiles in the mixture of helium and argon. As can be evident, the discharges studied in Refs. 7–10 consists of the cathode layer of width 1.8 mm and nonhomogeneous negative glow with low electron temperature T_e (see Fig. 6). Notice that the model reproduces such a subtle phenomenon as the field reversal.[24] It occurs at the point where the plasma density reaches its maximum value.[24–26] Anode drop, which is as small as several electron temperatures, is negative so that from this point on the ions move towards the anode.

Figure 7 shows the electron and ion density profiles over the discharge gap. As can be seen, the layer of ion volume charge is built up near the cathode, while the plasma is quasi neutral. Maximum of plasma density locates nearly at the middle of negative glow of plasma region.

Higher electron and ion temperatures are observed in the cathode layer of volume charge with strong electric field (see Fig. 6). In the plasma of negative glow, where electric field is weak (and may even be reversed), electron temperature is low and makes up tenth fractions of eV. Temperature

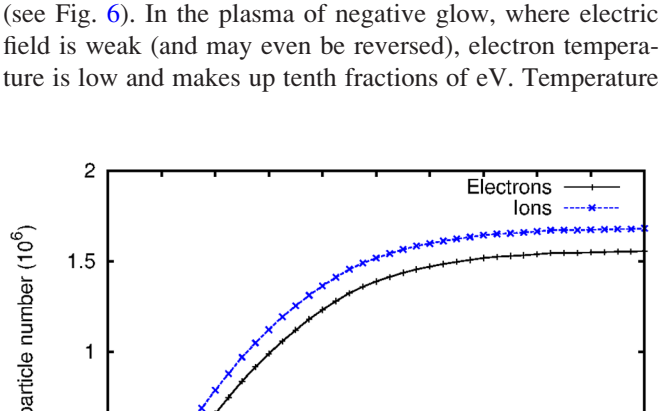

FIG. 4. Convergence test: number of super electrons and ions versus the time step. Conditions are given in Table III.

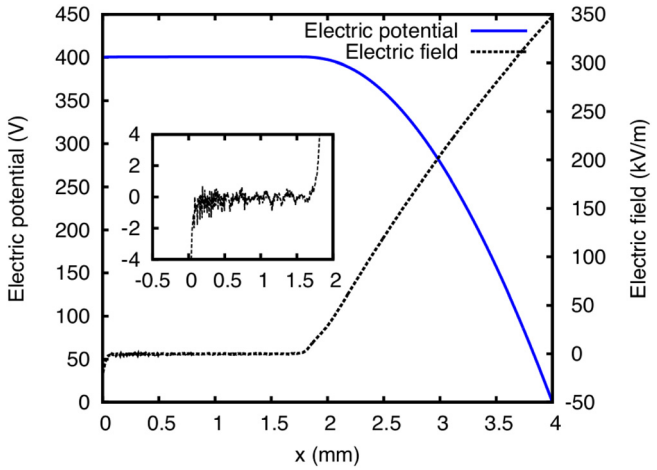

FIG. 5. Electric potential and field in the He-Ar mixture. Conditions are given in Table III.

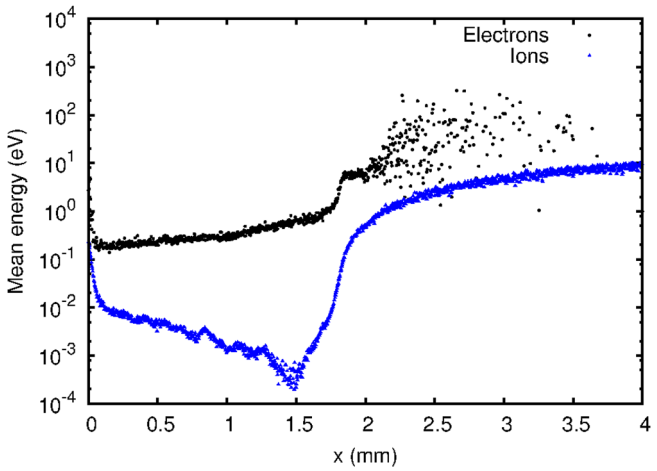

FIG. 6. Electron and helium ion mean energies in the He-Ar mixture.

of ions in the plasma is close to the room temperature due to effective heat exchange with neutral particles.

The helium ion EDF (see Fig. 8) in the cathode layer is distinctly different from that in the plasma region. In the cathode layer, the extensive continuous spectrum of ion EDF is clearly pronounced. It is formed by the accelerated in the strong field of cathode layer fast ions, recharging in the collisions with atoms. In the plasma, the ion EDF is close to Maxwellian with ions being at room temperature.

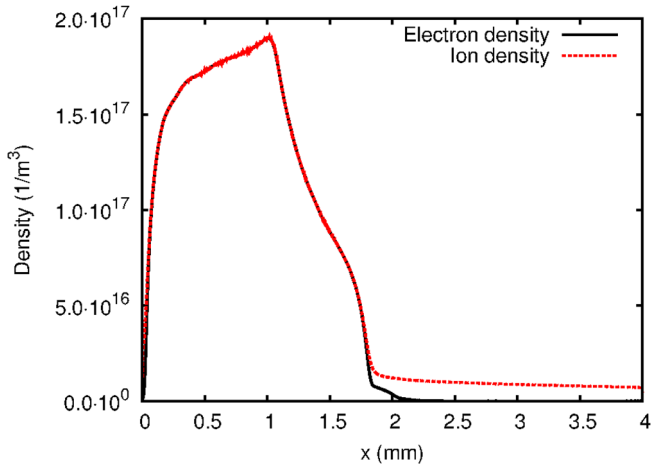

FIG. 7. Electron and helium ion density in the He-Ar mixture. Conditions are the same as in Fig. 5.

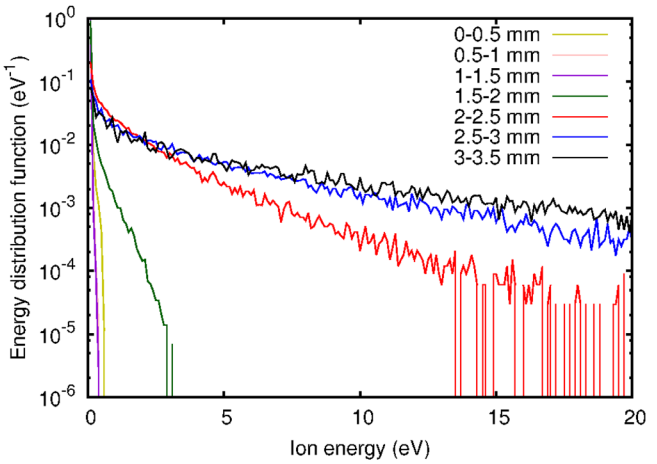

FIG. 8. Helium ion EDF's obtained in the He-Ar mixture. Conditions are the same as in Fig. 5.

Figure 9 shows EEDF in the discharge in the mixture of helium and argon. As evident from this figure, EEDF consists of the low-temperature Maxwellian part due to trapped electrons in the region of low energies and the high-energy tail due to fast (free) electrons. Spectrum of EDF of fast electrons is continuous. It is built up as a result of energy degradation in the course of the ionization and excitation processes by fast electrons, accelerated in the strong field of the cathode fall. The peaks due to Penning electrons, released in the reactions of metastable helium atoms with argon atoms (13) and (14), clearly stand out above the continuous spectrum at about 4.06 and 4.85 eV, as well as in the measured EEDF in Ref. 7. The peaks in the EEDF indicate the energies of the Penning electrons, from which, given the excitation energy of the working gas atoms and the ionization energy of the impurity atoms, the sort of the impurity can be obviously identified.

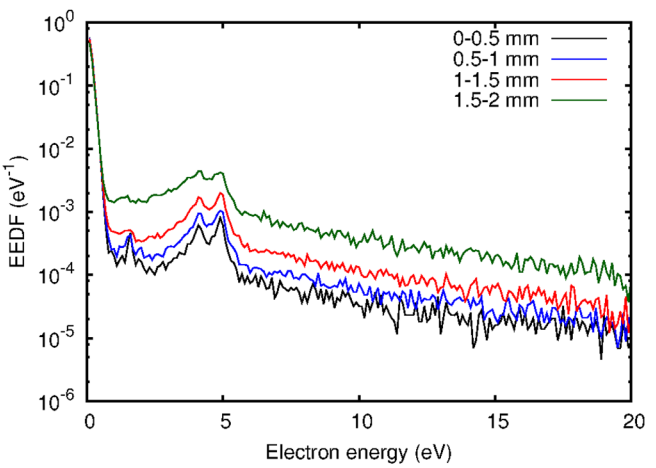

FIG. 9. EEDF's obtained in the He-Ar mixture. Conditions are the same as in Fig. 5.

IV. CONCLUSIONS

We performed Particle in Cell/Monte Carlo Collision (PIC/MCC) analysis related to the problem of detection and identification of impurities in the gas by the Plasma Spectroscopy (PLES) method.

The progress in the PLES requires development of the reliable numerical models and carrying out numerical simulations to gain better understanding of the applicability and limitations of this method and optimization of its performance. To this purpose, we developed 1*d*3*v* PIC/MCC code for simulations of glow discharges with nonlocal plasma. First, the code was verified under the conditions of RF capacitively coupled discharge in helium. Then, we parallelized the code using Open MPI. The effect of the parallelization on the performance of the code was studied as a function of the number of cores involved in the computations. Test calculations showed that the efficiency of the code increases about 70 times with increase of the number of cores up to 95.

As a demonstration of the PLES method, we carried out parallel PIC/MCC simulations of plasma of the DC glow discharge in helium doped by the small amount of argon. In this analysis, most attention was concentrated on the detection of a small (compared to the density of bulk electrons) fraction of fast (untrapped) electrons, which were released in the Penning ionization reactions between metastable atoms of the buffer gas and impurity. Computed results are consistent with those obtained in the experiments.[7–10] Indeed, computed EEDF revealed sharp peaks exactly at the release energies of the electrons, emerged in the Penning reactions.

ACKNOWLEDGMENTS

The work was supported by the joint research grant from the Scientific and Technical Research Council of Turkey (TUBITAK) 212T164 and Russian Foundation for Basic Research (RFBR). A.A.K. thanks RNF (Grant No. 14-19-00311) for the support. The simulations were performed using High Performance and Grid Computing Center (TRUBA Resources) at TUBITAK ULAKBIM.

[1]A. Bogaerts, E. Neyts, R. Gijbels, and J. Mullen, Spectrochim. Acta Part B **57**, 609 (2002).
[2]H. Kim, F. Iza, S. Yang, M. Radmilović-Radjenović, and J. Lee, J. Phys. D: Appl. Phys. **38**, R283 (2005).
[3]L. Tsendin, Plasma Sources Sci. Technol. **4**, 200 (1995).
[4]R. Arslanbekov and A. Kudryavtsev, Phys. Rev. E **58**, 6539 (1998).
[5]R. Arslanbekov and A. Kudryavtsev, Phys. Plasmas **6**, 1003 (1999).
[6]N. Kolokolov and A. Kudrjavtsev, Phys. Scr. **50**, 371 (1994).
[7]M. Stefanova, P. Pramatarov, A. Kudrjavtsev, and R. Peyeva, J. Phys. Conf. Ser. **514**, 012052 (2014).
[8]A. Kudryavtsev, M. Stefanova, and P. Pramatarov, Phys. Plasmas **22**, 103513 (2015).
[9]A. Kudryavtsev, P. Pramatarov, M. Stefanova, and N. Khromov, J. Instrum. **7**, P07002 (2012).
[10]A. Kudryavtsev, M. Stefanova, and P. Pramatarov, J. Appl. Phys. **117**, 133303 (2015).
[11]E. Kawamura, C. K. Birdsall, and V. Vahedi, Plasma Sources Sci. Technol. **9**, 413 (2000).
[12]H. Skullerud, J. Phys. D: Appl. Phys. **1**, 1567 (1968).
[13]J. J. J. Blahovec, L. A. Bowers, J. W. Luginsland, G. E. Sasser, and J. J. Watrous, IEEE Trans. Plasma Sci. **28**, 821 (2000).
[14]P. C. Liewer and V. K. Decyk, J. Comput. Phys. **85**, 302 (1989).
[15]B. D. Martino, S. Briguglio, G. Vlad, and P. Sguazzero, Parallel Comput. **27**, 295 (2001).
[16]See www.lxcat.net for "Biagi-v7.1 (magboltz version 7.1)" (last accessed 18 February 2016).
[17]J. Verboncoeur, Plasma Phys. Controlled Fusion **47**, A231 (2005).
[18]Z. Donko, Plasma Sources Sci. Technol. **20**, 024001 (2011).
[19]M. Turner, A. Derzsi, Z. Dónko, D. Eremin, S. J. Kelly, T. Lafleur, and T. Mussenbrock, Phys. Plasmas **20**, 013507–1 (2013).
[20]See http://jilawww.colorado.edu/~avp/collision_data/ionneutral/IONATOM.TXT for "Cross sections for collisions of He^+ with He and Ar^+ with He" (last accessed 16 June 2014).
[21]S. Goedecker and A. Hoisiye, *Performance Optimization of Numerically Intensive Codes* (Society for Industrial and Applied Mathematics, 2001).
[22]Q. Wang, D. J. Economou, and V. M. Donnelly, J. Appl. Phys. **100**, 023301 (2006).
[23]A. L. Schmeltekopf and F. C. Fesenfeld, J. Chem. Phys. **53**, 3173 (1970).
[24]J. Boeuf and L. Pitchford, J. Phys. D **28**, 2083 (1995).
[25]I. Rafatov, E. Bogdanov, and A. Kudryavtsev, Phys. Plasmas **19**, 033502 (2012).
[26]E. Eylenceoglu, I. Rafatov, and A. Kudryavtsev, Phys. Plasmas **22**, 013509 (2015).